J|A|C|S
COMMUNICATIONS

Published on Web 06/06/2002

Enantioselective Guest Exchange in a Chiral Resorcin[4]arene Cavity

Bruno Botta, Maurizio Botta,† Antonello Filippi, Andrea Tafi,† Giuliano Delle Monache,‡ and Maurizio Speranza*

Dipartimento degli Studi di Chimica e Tecnologia delle Sostanze Biologicamente Attive, Università "La Sapienza", 00185 Roma, Italy

Received February 14, 2002

Chiral recognition by artificial enzymes is one of the most challenging topics in biochemistry, pharmaceuticals, and catalysis. Enantioselectivity in these systems is due to shape-specific noncovalent attractive and repulsive interactions between a chiral guest molecule and the chiral cavity of the receptor. The driving force for the formation of host−guest inclusion complexes in aqueous solution is the so-called "hydrophobic effect",[1−5] due to the expulsion of solvent molecules from the receptor cavity after desolvation and incorporation of a hydrophobic guest. Thus, the solvent plays a considerable role in enantioselective host/guest complexation in solution and complicates the understanding of the underlying principles. These difficulties can be removed by studying chiral recognition under solvent-free conditions. A variety of ionic inclusion complexes with cyclodextrins,[6] cytochrome *c*,[7] and crown ethers[8] as chiral hosts have been generated in the gas phase and the effects of the guest configuration thoroughly investigated.

In this work another category of potential artificial enzymes has been considered, that is, resorcin[4]arenes, which are synthetic macrocycles with a cavity-shaped very flexible architecture. In particular, the chiral amido[4]resorcinarene $\mathbf{1_L}$ (Figure 1; R = Et) was chosen as a model, whose molecular asymmetry is due to the four axial pendants containing the chiral L-valine group. The intrinsic enantioselectivity of the $\mathbf{1_L}$ host was checked by generating in the gas-phase its proton-bonded complexes with several representative amino acids (A), such as D- and L-alanine and D- and L-serine, and by measuring the exchange rate of A with (*S*)-(+)- and (*R*)-(−)-2-butylamine (B) (eq 1).

$$[\mathbf{1_L}\cdot H\cdot A]^+ + B \rightarrow [\mathbf{1_L}\cdot H\cdot B]^+ + A \qquad (1)$$

Optically pure $\mathbf{1_L}$ was synthesized and purified according to established procedures.[9] Stock solutions of $\mathbf{1_L}$ (1×10^{-5} M) in H_2O/CH_3OH = 1:3, containing a 5-fold excess of the appropriate amino acid A, were electrosprayed through a heated capillary (130 °C) into the external source of a Fourier transform ion cyclotron resonance mass spectrometer (FT-ICR-MS) and the resulting positive ions transported into the analyzer cell. Abundant signals, corresponding to the natural isotopomers of the proton-bound complex $[\mathbf{1_L}\cdot H\cdot A]^+$, were monitored and isolated by broad-band ejection of the accompanying ions. When a background pressure of $(2-6) \times 10^{-8}$ mbar of either (*S*)-(+)- or (*R*)-(−)-2-butylamine (B) was introduced in the FT-ICR-MS cell,[10] the exchange reaction 1 exclusively takes place. The appearance of the exchanged product $[\mathbf{1_L}\cdot H\cdot B]^+$ was monitored as a function of time.

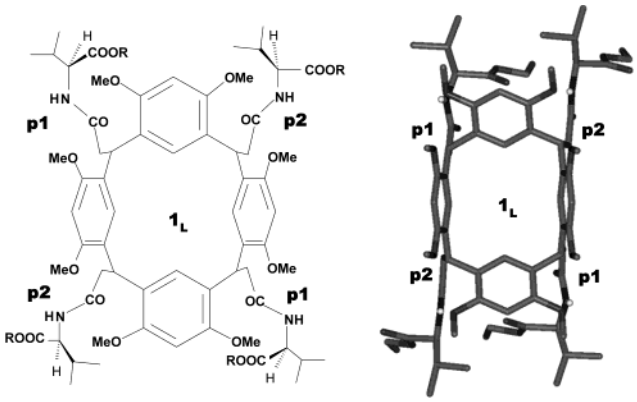

Figure 1. Formula and top view (R = ethyl) of a local minimum-geometry for the flattened-cone conformation of $\mathbf{1_L}$. Symmetrically equivalent chiral pendants are labeled with the same symbol, either p1 or p2.

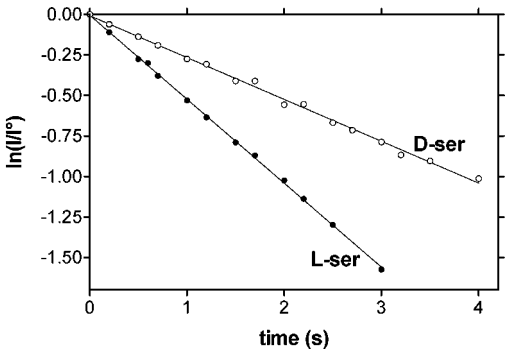

Figure 2. Kinetic plots for the gas-phase reaction between (*S*)-(+)-2-butylamine ($P = 2.8 \times 10^{-8}$ mbar) and $[\mathbf{1_L}\cdot H\cdot A]^+$ (A = D-serine (r^2 = 0.996); A = L-serine (r^2 = 0.999)).

Rate constants *k* of reaction 1 were obtained from the slopes of the pseudo-first-order rate plots ($\ln(I/I_0)$ vs *t*), where *I* is the intensity of complex $[\mathbf{1_L}\cdot H\cdot A]^+$ at the delay time *t* and I_0 is the sum of the intensities of $[\mathbf{1_L}\cdot H\cdot A]^+$ and $[\mathbf{1_L}\cdot H\cdot B]^+$. Representative rate plots are given in Figure 2.

Table 1 reports the relevant *k* values, measured as a function of the configuration of A and B. Its inspection reveals that reaction 1 is efficient (Table 1, figures in parentheses) and enantioselective (k_D/k_L). Irrespective of the configuration of amine B, D-alanine is released faster than L-alanine ($k_D/k_L > 1$). The reverse is true when the leaving amino acid is a serine enantiomer ($k_D/k_L < 1$). The alanine complexes display the highest enantioselectivity in the reaction with (*R*)-(−)-2-butylamine ($k_D/k_L = 1.5 \pm 0.1$), whereas the same reaction on the serine complexes exhibits the lowest selectivity ($k_D/k_L = 0.7 \pm 0.1$). The relative reactivity of diastereomeric pairs depends on the configuration of the incoming

* To whom correspondence should be addressed. E-mail: maurizio.speranza@uniroma1.it.
† Dipartimento Farmaco Chimico Tecnologico, Università di Siena, 53100 Siena, Italy.
‡ Istituto Chimica del Riconoscimento Molecolare, Università Cattolica del Sacro Cuore, 00168 Roma, Italy.

10.1021/ja020232t CCC: $22.00

Table 1. Exchange Rate Constants[a]

2-butyl amine (B)	amino acid (A) D-ala k_D	L-ala k_L	k_D/k_L	amino acid (A) D-ser k_D	L-ser k_L	k_D/k_L
(*R*)-(−)	7.7(0.69)	5.0(0.45)	1.5 ± 0.1	4.6(0.41)	6.9(0.62)	0.7 ± 0.1
(*S*)-(+)	7.1(0.63)	5.9(0.53)	1.2 ± 0.1	3.8(0.34)	7.6(0.68)	0.5 ± 0.1
k_R/k_S	1.1 ± 0.1	0.8 ± 0.1		1.2 ± 0.1	0.9 ± 0.1	

[a] k x 10^{10} cm^3 molecule^{-1} s^{-1}; the values in parentheses represent the reaction efficiencies given as the ratio between the measured rate constants and the corresponding collision constant, calculated from the trajectory calculation method (Su, T.; Chesnavitch, W. J. *J. Chem. Phys.* **1982**, *76*, 5183).

2-butylamine B as well. Thus, (*R*)-(−)-2-butylamine reacts faster than the (*S*)-enantiomer with $[\mathbf{1_L}\cdot H\cdot A]^+$ containing the D-amino acids ($k_R/k_S > 1$). The reverse is true with the L-amino acids ($k_R/k_S < 1$).

The enantioselectivity picture emerging from Table 1 cannot be simply rationalized in terms of the relative stability of the diastereomeric forms of either $[\mathbf{1_L}\cdot H\cdot A]^+$ and $[\mathbf{1_L}\cdot H\cdot B]^+$ (vide infra). Rather, it must be related to the effects of the resorcin[4]-arene frame upon the transition structures involved in the exchange reaction 1. However, even a qualitative outlook of these transition structures presents some problems, since they may depend on the actual proton-bonding site in $[\mathbf{1_L}\cdot H\cdot A]^+$ as well as on the mutual orientation of the leaving A and incoming B molecules relative to the host, whether both inside or outside its cavity or one inside and the other outside.

Some indications about the nature of proton bonding in $[\mathbf{1_L}\cdot H\cdot A]^+$ can be obtained from their sustained off-resonance collision-induced decomposition (SORI−CID). Indeed, exclusive detection of the $[\mathbf{1_L}\cdot H]^+$ fragment from these experiments suggests that, in the $[\mathbf{1_L}\cdot H\cdot A]^+$ complex, the proton is more strongly bonded to the resorcin[4]arene host, most probably to the CO oxygen of one of its amido groups,[11] rather than to the guest.

BatchMin Monte Carlo multiple minimum methodology (MCMM) simulations of the proton-bound complexes between $\mathbf{1_L}$ (R = Me)[12] and the alanine enantiomers provide some information about their most probable structure. The complexes were reproduced by two flexible docking experiments following an already described and validated protocol.[13] In compliance with the SORI-CID results and literature indications,[11] input geometries of $\mathbf{1_L}$ protonated at either **p1** or **p2** amido group were used (Figure 1). Irrespective of the input protonation site, the docking results point to a single $[\mathbf{1_L}\cdot H]^+$ structure with the proton invariably located at position **p2** of the host. The structure is rather rigid because of the presence of a network of hydrogen bonds involving the four axial pendants. Two regions of $[\mathbf{1_L}\cdot H]^+$ proved to be best suited for accommodating the alanine enantiomers, one inside the achiral upper rim (**up**) and the other around the chiral lower one (**lo**). Molecular dynamics simulations at 300 K, performed on both the MCMM-determined docking geometries, point to this latter region as the most favored one, as demonstrated by the difference between the computed average potential energy of **up** and **lo** ($\Delta H_{300} = \sim 4$ kcal mol^{-1}). The alanine guest is best accommodated between the protonated **p2** and the **p1** amido groups of the host (Figure 3). In the $[\mathbf{1_L}\cdot H\cdot$ L-ala$]^+$ structure, the amino group of L-ala is H-bonded to protonated **p2** and to the CO oxygen of the estereal group at **p1**. A third H-bond is formed between the COOH of L-ala and the CO oxygen of the amido group at **p1**. In the $[\mathbf{1_L}\cdot H\cdot$D-ala$]^+$ structure, the amino group of D-ala is H-bonded to protonated **p2** and to the CO oxygen of the amido group at **p1**. A third H-bond is established between the COOH of alanine and to the CO oxygen of the estereal group at **p1**. Both structural arrangements push the alanine methyl group outward from the host frame.

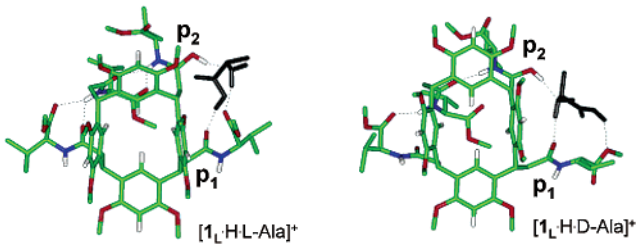

Figure 3. Top view of one of the inclusion complexes $[\mathbf{1_L}\cdot H\cdot$L-ala$]^+$ and $[\mathbf{1_L}\cdot H\cdot$D-ala$]^+$. The guest molecule (in black) is hosted at the lower chiral rim of $\mathbf{1_L}$. Hydrogen-bonding interactions are depicted as dotted lines.

These preliminary results point to chiral resorcin[4]arenes as very promising tools for further chiral recognition studies in the gas phase. The investigation of the factors governing enantiodiscrimination in these systems, in the absence of complicating solvation/desolvation phenomena, is expected to be of great interest in modeling enzymatic catalysis.

Acknowledgment. Work is supported by the Ministero dell'Istruzione dell'Università e della Ricerca (MIUR) and the Consiglio Nazionale delle Ricerche (CNR). M.S. and A.F. express their gratitude to F. Angelelli for technical assistance.

Supporting Information Available: Computational details (PDF). This material is available free of charge via the Internet at http://pubs.acs.org.

References

(1) Diedrich, F. *Angew. Chem., Int. Ed. Engl.* **1988**, *27*, 362.
(2) Lehn, J. M. *Angew. Chem., Int. Ed. Engl.* **1988**, *27*, 89.
(3) Cram, D. *Angew. Chem., Int. Ed. Engl.* **1988**, *27*, 1009.
(4) Jeong, K. S.; Rebek, J. *J. Am. Chem. Soc.* **1988**, *110*, 3327 and references therein.
(5) Pant, N.; Hamilton, A. D. *J. Am. Chem. Soc.* **1988**, *110*, 2002.
(6) For comprehensive reviews, see: (a) Ahn, S.; Ramirez, J.; Grigorean, G.; Lebrilla, C. B. *J. Am. Soc. Mass Spectrom.* **2001**, *12*, 278. (b) Lebrilla, C. B.. *Acc. Chem. Res.* **2001**, *34*, 653.
(7) Camara, E.; Green, M. K.; Penn, S. G.; Lebrilla, C. B. *J. Am. Chem. Soc.* **1996**, *118*, 8751.
(8) For comprehensive reviews, see: (a) Dearden, D. V.; Liang, Y.; Nicoll, J. B.; Kellersberger, K. A. *J. Mass Spectrom.* **2001**, *36*, 989. (b) Sawada, M. *Mass Spectrom. Rev.* **1997**, *16*, 73.
(9) Botta, B.; Delle Monache, G.; Salvatore, P.; Gasparrini, F.; Villani, C.; Botta, M.; Corelli, F.; Tafi, A.; Gacs-Baitz, E.; Santini, A.; Carvalho, C.; Misiti, D. *J. Org. Chem.* **1997**, *62*, 932.
(10) Accurate determination of the B pressure was carried out after careful calibration of the ion gauge of the instrument (Bartmess, J. E.; Georgiadis, R. M. *Vacuum* **1983**, *33*, 149).
(11) Bagno, A. *J. Phys. Org. Chem.* **2000**, *13*, 574.
(12) Calculations using the AMBER* force field as implemented in Macro-Model 5.5 (Mohamadi, F.; Richards, N. G. J.; Guida, W. C.; Liskamp, R.; Lipton, M.; Caufield, C.; Chang, G.; Hendrickson, T.; Still, W. C.. *J. Comput. Chem.* **1990**, *11*, 440). The methylated analogue of $\mathbf{1_L}$ was taken into account to reduce the calculation size.
(13) Tafi A.; van Almsick, A.; Corelli, F.; Crusco, M.; Laumen, K. E.; Schneider, M. P.; Botta, M. *J. Org. Chem.* **2000**, *65*, 3659.

JA020232T